electronics

MDPI

Article

Hybrid Beamforming for Millimeter-Wave Heterogeneous Networks

Mostafa Hefnawi

Department of Electrical and Computer Engineering, Royal Military College of Canada, Kingston, ON K7K 7B4, Canada; hefnawi@rmc.ca

Received: 23 December 2018; Accepted: 23 January 2019; Published: 28 January 2019

Abstract: Heterogeneous networks (HetNets) employing massive multiple-input multiple-output (MIMO) and millimeter-wave (mmWave) technologies have emerged as a promising solution to enhance the network capacity and coverage of next-generation 5G cellular networks. However, the use of traditional fully-digital MIMO beamforming methods, which require one radio frequency (RF) chain per antenna element, is not practical for large-scale antenna arrays, due to the high cost and high power consumption. To reduce the number of RF chains, hybrid analog and digital beamforming has been proposed as an alternative structure. In this paper, therefore, we consider a HetNet formed with one macro-cell base station (MBS) and multiple small-cell base stations (SBSs) equipped with large-scale antenna arrays that employ hybrid analog and digital beamforming. The analog beamforming weight vectors of the MBS and the SBSs correspond to the the best-fixed multi-beams obtained by eigendecomposition schemes. On the other hand, digital beamforming weights are optimized to maximize the receive signal-to-interference-plus-noise ratio (SINR) of the effective channels consisting of the cascade of the analog beamforming weights and the actual channel. The performance is evaluated in terms of the beampatterns and the ergodic channel capacity and shows that the proposed hybrid beamforming scheme achieves near-optimal performance with only four RF chains while requiring considerably less computational complexity.

Keywords: hybrid beamforming; massive MIMO; HetNets; mmWaves

1. Introduction

Recently, heterogeneous networks (HetNets) that use massive multiple-input multiple-output (MIMO) and millimeter-wave (mmWave) technologies has emerged as a promising solution to enhance the network capacity and coverage of next-generation 5G cellular networks [1–6]. Small cell deployment in HetNets can achieve high signal to interference plus noise ratio (SINR) and dense spectrum reuse, mmWave can address the current challenge of bandwidth shortage, and the large number of antenna arrays [7–10] are essential for mmWaves to compensate for channel attenuation. In Reference [11] we applied the concept of massive multiuser (MU)-MIMO to enhance both the access and the backhaul links in HetNets, and it was shown that such a concept could significantly improve the system performance in terms of link reliability, spectral efficiency, and energy efficiency. Traditional MIMO-beamforming systems require a dedicated radio frequency (RF) chain for each antenna element, which becomes impractical with massive MIMO systems due to either cost or power consumption. To reduce the number of RF chains, hybrid beamforming (HBF), which combines RF analog and baseband digital beamformers, has been proposed as a promising solution [12–17]. Figure 1 shows a general hybrid configuration that connects N_a antenna elements to N_d RF chains, where $N_d < N_a$, using an analog RF beamforming matrix built from only phase-shifters. Two widely-used analog beamformer architectures for hybrid beamforming are shown in Figure 2. The fully-connected hybrid beamforming structure of Figure 2a provides a full beamforming gain per transceiver—but with

high complexity—by connecting each RF chain to all antennas through a network of $N_d \times N_a$ phase shifters [12–15]. Figure 2b, on the other hand, shows a partially-connected structure, where each RF chain is connected to N_a / N_d number of sub-arrays. Such a structure has a lower hardware complexity at the price of reduced beamforming gain.

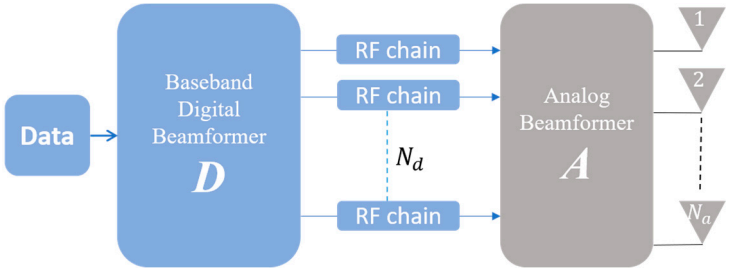

Figure 1. Hybrid beamforming.

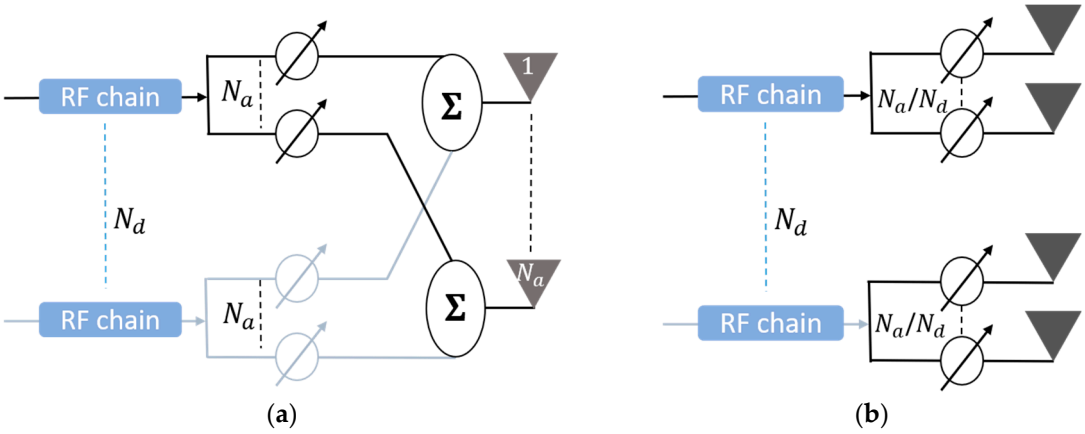

Figure 2. The architecture of analog beamformers: (**a**) Fully-connected structure; (**b**) partially-connected structure.

Previous studies on massive hybrid MIMO mainly focused on single-user systems [12–14]. On the other hand, MU-MIMO cases were studied in References [15–17]. In Reference [15] a scheme called Joint Spatial Division Multiplexing (JSDM) was proposed to create multiple virtual sectors which reduce the overhead and computational complexity of downlink training and uplink feedback. In References [16,17] it was shown that the required number of RF chains only needs to be twice the number of data streams to achieve the same performance of any fully-digital beamforming scheme. These studies, however, did not consider HBF in the context of HetNets and focused primarily on macro-cellular systems. In this paper, we consider a HetNet where both the macro-cell base stations (MBSs) and small-cell base stations (SBSs) are equipped with fully-connected massive hybrid antenna arrays, while all mobile users have a single antenna. We propose a low-complexity HBF that is fully-based on eigenbeamforming. The MBSs and the SBSs select the best-fixed multi-beams by eigendecomposition of the access and backhaul channels. The selected beams are then used by the digital beamformers, which are based on the maximization of the receive SINR of the effective channels consisting of the cascade of the analog beamforming weights and the actual channel [18,19].

2. System Model

We consider the access and backhaul uplinks in the HetNet of Figure 3, where K cognitive small cells and their L_s small-cell users (SUs) are concurrently sharing the same frequency band with one MBS and their L_p macro-cell primary users (PUs). It is assumed that both the MBS and SBSs are equipped with massive hybrid antenna arrays while the SUs and PUs are equipped with a single

antenna. The SBSs are acting as smart relays between the SUs and the MBS with N_a- element transmitting/receiving antenna arrays and N_d RF chains. The MBS is equipped with M_a- element antenna arrays and M_d RF chains. It is also assumed that both the SBS and the MBS perform an OFDM-based transmission and that the analog beamformers are identical for all subcarriers while adapting digital beamformers in each subcarrier.

Let $\boldsymbol{x}_s[f_n] = \left\{x_1^s, x_2^s, \cdots, x_{L_s}^s\right\}$ and $\boldsymbol{x}_p[f_n] = \left\{x_1^p, x_2^p, \cdots, x_{L_p}^p\right\}$ denote, respectively, the set of L_s SUs signals and L_p PUs signals transmitted on each subcarrier, and f_n, $n = 1, \cdots, N_c$, where N_c denotes the number of subcarriers per OFDM symbol in the system. The analysis is done separately on each subcarrier. For brevity therefore, we drop the frequency index f_n.

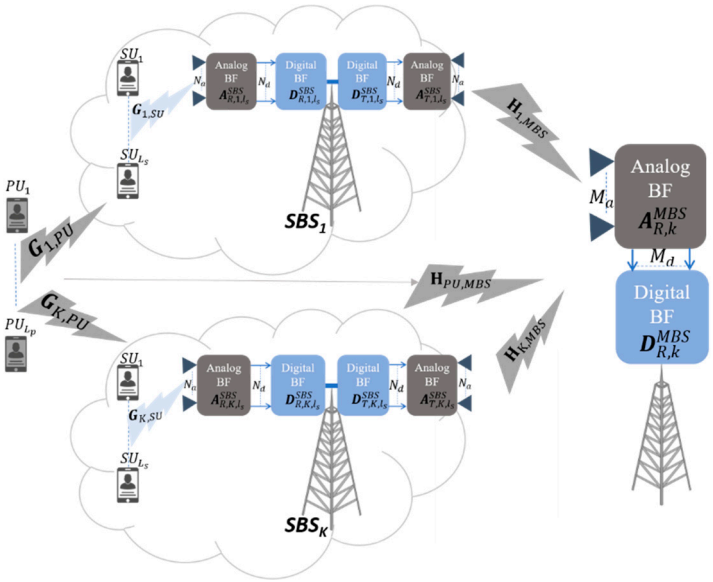

Figure 3. System model: hybrid beamforming-based HetNet with one macro-cell and K small-cells.

2.1. Access Link

The $N_a \times 1$ received signal vector $\boldsymbol{y}_{k,SBS}$ at the k^{th} SBS is given by

$$\boldsymbol{y}_{k,SBS} = \boldsymbol{G}_{k,SU}\boldsymbol{x}_s + \boldsymbol{G}_{k,PU}\boldsymbol{x}_p + \boldsymbol{n}_{k,SBS}, \tag{1}$$

where $\boldsymbol{G}_{k,SU} \in \mathbb{C}^{N_a \times L_s}$ is the channel matrix between the k^{th} SBS and its L_s users, $\boldsymbol{G}_{k,PU} \in \mathbb{C}^{N_a \times L_p}$ is the channel matrix between the k^{th} SBS and the L_p PUs, $\boldsymbol{x}_s \in \mathbb{C}^{L_s \times 1}$ is the transmitted signal vector of L_s users in the k^{th} small-cell, $\boldsymbol{x}_p \in \mathbb{C}^{L_p \times 1}$ is the transmitted signal vector of L_p users in the HetNet, and $\boldsymbol{n}_{k,SBS} \in \mathbb{C}^{N_a \times 1}$ is the received complex additive white Gaussian noise (AWGN) vector at the k^{th} SBS.

It should be noted that in Equation (1), the interference between small-cells was neglected. This was justified by the fact that small-cell base stations are using a large number of antennas, which enables sharp beamforming towards their users without harming neighboring small-cells.

The k^{th} SBS received signal, $\boldsymbol{y}_{k,SBS}$, is first applied to an $N_a \times N_d$ receive analog beamforming weight matrix, $\boldsymbol{A}_{R,k,l_s}^{SBS}$, whose output is directed to an $N_d \times N_d$ receive digital beamforming weight vector $\boldsymbol{D}_{R,k,l_s}^{SBS}$. If we denote the combined digital-analog receive beamformer for the l_s^{th} user as $\mathbf{w}_{R,k,l_s} = \boldsymbol{A}_{R,k,l_s}^{SBS}\boldsymbol{D}_{R,k,l_s}^{SBS}$, then the detection of the l_s^{th} user signal by its k^{th} SBS can be expressed as

$$\begin{aligned} \boldsymbol{r}_{k,l_s} &= \mathbf{w}_{R,k,l_s}^{\mathrm{H}}\boldsymbol{y}_{k,SBS} = \mathbf{w}_{R,k,l_s}^{H}\boldsymbol{G}_{k,SU}\boldsymbol{x}_s + \mathbf{w}_{R,k,l_s}^{H}\boldsymbol{G}_{k,PU}\boldsymbol{x}_p + \mathbf{w}_{R,k,l_s}^{H}\boldsymbol{n}_{k,SBS} \\ &= \mathbf{w}_{R,k,l_s}^{H}\boldsymbol{g}_{k,l_s}x_{l_s}^s + \mathbf{w}_{R,k,l_s}^{H}\sum_{i=1,i\neq l_s}^{L_s}\boldsymbol{g}_{k,i}x_i^s + \mathbf{w}_{R,k,l_s}^{H} + \boldsymbol{G}_{k,PU}\boldsymbol{x}_p + \mathbf{w}_{R,k,l_s}^{H}\boldsymbol{n}_{k,SBS} \end{aligned} \tag{2}$$

where $\boldsymbol{g}_{k,l_s}$ is the l_s^{th} column of $\boldsymbol{G}_{k,SU}$ that represents the channel between the k^{th} SBS and its l_s^{th} user.

If we denote $\mathbf{H}_{AL,k,l_s} = \left(\boldsymbol{A}_{R,k,l_s}^{SBS}\right)^H \boldsymbol{g}_{k,l_s}$ as the effective access channel between the k^{th} SBS and its l_s^{th} user, then for a set of selected beams, i.e. known $\left(\boldsymbol{A}_{R,k,l_s}^{SBS}\right)^H$, the SINR can be expressed in terms of the digital beamformer, $\boldsymbol{D}_{R,k,l_s}^{SBS}$, as

$$\gamma_{k,l_s}^{SBS} = \frac{\left(\boldsymbol{D}_{R,k,l_s}^{SBS}\right)^H \mathbf{H}_{AL,k,l_s} x_{l_s}^s \left(x_{l_s}^s\right)^H \mathbf{H}_{AL,k,l_s}^H \boldsymbol{D}_{R,k,l_s}^{SBS}}{\left(\boldsymbol{D}_{R,k,l_s}^{SBS}\right)^H \mathbf{B}_{AL} \boldsymbol{D}_{R,k,l_s}^{SBS}} \ , \tag{3}$$

where $\mathbf{B}_{AL}$ is the covariance matrix of the interference-plus-noise given by

$$\mathbf{B}_{AL} = \underbrace{\sum_{i=1, i\neq l_s}^{L_s} \left(\boldsymbol{A}_{R,k,i}^{SBS}\right)^H \boldsymbol{g}_{k,i} x_i^s (x_i^s)^H \boldsymbol{g}_{\mathrm{k,i}}^H \boldsymbol{A}_{R,k,i}^{SBS}}_{\text{Interference from } L_s-1 \text{ SUs}} + \underbrace{\left(\boldsymbol{A}_{R,k,l_s}^{SBS}\right)^H \boldsymbol{G}_{k,PU} \boldsymbol{x}_p \boldsymbol{x}_p^H \boldsymbol{G}_{\mathrm{k,PU}}^H \boldsymbol{A}_{R,k,l_s}^{SBS}}_{\text{Interference from } L_p \text{ PUs}} + \sigma_n^2 (\boldsymbol{A}_{R,k,l_s}^{SBS}) \boldsymbol{A}_{R,k,l_s}^{SBS}, \tag{4}$$

2.2. Backhaul Link

The hybrid beamforming weights at the backhaul link are obtained based on orthogonal pilot signals transmitted from each SBS to the MBS. The k^{th} SBS applies its pilot signal $\boldsymbol{s}_k^p \in \mathbb{C}^{N_d \times 1}$ to an $N_d \times N_d$ transmit digital beamforming weight vector $\boldsymbol{D}_{T,k}^{SBS}$ followed by an $N_a \times N_d$ transmit analog beamforming matrix $\boldsymbol{A}_{T,k}^{SBS}$. If we denote the combined digital-analog transmit beamformer for the k^{th} SBS as $\mathbf{w}_{T,k} = \boldsymbol{A}_{T,k}^{SBS} \boldsymbol{D}_{T,k}^{SBS}$, then the array output of the MBS can be written as

$$\boldsymbol{y}_{\text{MBS}}^p = \sum_{k=1}^{K} \mathbf{H}_{k,MBS} \mathbf{w}_{T,k} s_k^p + \mathbf{H}_{PU,MBS} x_p + \boldsymbol{n}_{MBS} \ , \tag{5}$$

where $\boldsymbol{y}_{\text{MBS}}^p$ is the $M_a \times 1$ vector containing the outputs of the M_a- element antenna array of the MBS, $\mathbf{H}_{k,MBS}$ is the $N_a \times M_a$ channel matrix representing the transfer functions from the N_a- element antenna array of the k^{th} SBS to the M_a- element antenna array of the MBS, $\mathbf{H}_{PU,MBS}$ is the $M_a \times L_{\text{p}}$ channel matrix from the L_p PUs to the MBS's M_a- element antenna array, and $\mathbf{n}_{MBS}$ is the received $M_a \times 1$ complex AWGN vector at the MBS.

The MBS detects the k^{th} SBS signal by applying the output of the array $\boldsymbol{y}_{\text{MBS}}^p$ to the $M_a \times M_d$ receive analog weight matrix $\boldsymbol{A}_{R,k}^{MBS}$ followed by the $M_d \times M_d$ receive digital beamforming weight vector $\boldsymbol{D}_{k,R}^{MBS}$. If we denote the combined digital-analog receive beamformer for the k^{th} SBS as $\boldsymbol{c}_k = \boldsymbol{A}_{k,R}^{MBS} \boldsymbol{D}_{k,R}^{MBS}$, then the detection of the k^{th} SBS signal by the MBS can be expressed as

$$\hat{\boldsymbol{x}}_k = \boldsymbol{c}_k^H \boldsymbol{y}_{\text{MBS}}^p = \boldsymbol{S}_k^p + \boldsymbol{S}_{I_k} + \boldsymbol{S}_{I_p} + c_k^H \boldsymbol{n}_{MBS} \ , \tag{6}$$

where $\boldsymbol{S}_k^p = \boldsymbol{c}_k^H \mathbf{H}_{k,MBS} \mathbf{w}_{T,k} \boldsymbol{s}_k^p$ is the k^{th} SBS signal, $\boldsymbol{S}_{I_k} = \boldsymbol{c}_k^H \sum_{i=1, i\neq k}^{K} \mathbf{H}_{k,MBS} \mathbf{w}_{T,k} \boldsymbol{s}_k^p$ is the interference from $K-1$ other SBSs, and $\boldsymbol{S}_{\boldsymbol{I_p}} = \boldsymbol{c}_k^H \mathbf{H}_{PU,MBS} \boldsymbol{x}_p$ is the interference from L_p PUs.

Assuming that $\boldsymbol{s}_k^p$ are complex-valued random variables with unit power, i.e., $E\left[\|\boldsymbol{s}_k^p\|^2\right] = 1$, and denoting $\mathbf{H}_{BL,k} = \left(\boldsymbol{A}_{R,k}^{MBS}\right)^H \mathbf{H}_{k,MBS} \left(\boldsymbol{A}_{T,k}^{SBS}\right)^H$ as the effective channel between the k^{th} SBS and the MBS, the SINR at the MBS for the k^{th} SBS can be expressed as

$$\gamma_k^{MBS} = \frac{\left(\boldsymbol{D}_{R,k}^{MBS}\right)^H \mathbf{H}_{BL,k} \left(\boldsymbol{D}_{T,k}^{SBS}\right)^H \boldsymbol{D}_{T,k}^{SBS} \mathbf{H}_{BL,k}^H \boldsymbol{D}_{R,k}^{MBS}}{\boldsymbol{c}_k^H \mathbf{B}_{BL} \boldsymbol{c}_k}, \tag{7}$$

where $\mathbf{B}_{BL} = \sum_{i=1,i\neq k}^{K} \mathbf{H}_{i,MBS}\mathbf{w}_{T,i}\mathbf{w}_{T,i}^{H}\mathbf{H}_{i,MBS}^{H} + \mathbf{H}_{PU,MBS}\boldsymbol{x}_p\boldsymbol{x}_p^{H}\mathbf{H}_{PU,MBS}^{H} + \sigma_n^2\mathbf{I}_{M_a}$ is the covariance matrix of the interference-plus-noise at the backhaul link.

2.3. End-to-End SINR and Channel Capacity

Once the hybrid beamforming weights of the backhaul link are obtained, they can be used to forward the SUs signals to the MBS. The k^{th} SBS applies the received l_s^{th} user signal, $\mathbf{w}_{R,k,l_s}^{H}\boldsymbol{g}_{k,l_s}x_{l_s}^{s}$, to the hybrid beamformer, $\mathbf{w}_{T,k}$. The $N_{T,a} \times 1$ transmitted signal $\boldsymbol{s}_{k,l_s}$ at the output of the antenna array can then be expressed as

$$\boldsymbol{s}_{k,l_s} = \mathbf{w}_{T,k}\mathbf{w}_{R,k,l_s}^{H}\boldsymbol{g}_{k,l_s}x_{l_s}^{s}\ , \tag{8}$$

and the expression for the array output of the MBS can be written as

$$\boldsymbol{y}_{MBS} = \mathbf{H}_{PU,MBS}\boldsymbol{x}_p + \boldsymbol{y}_{k,MBS} + \sum_{i=1,\ i\neq k}^{K} \boldsymbol{y}_{i,MBS} + \boldsymbol{n}_{MBS}\ , \tag{9}$$

where $\boldsymbol{y}_{k,MBS} = \mathbf{H}_{k,MBS}\mathbf{w}_{T,k}\mathbf{w}_{R,k,l_s}^{H}\boldsymbol{y}_k$ is the array output of the MBS from the k^{th} SBS.

Using Equation (2), $\boldsymbol{y}_{k,MBS}$ can be expressed in terms of the l_s^{th} user signal, $x_{l_s}^{s}$, as follows:

$$\begin{aligned}\boldsymbol{y}_{k,MBS} &= \mathbf{H}_{k,MBS}\mathbf{w}_{T,k}\mathbf{w}_{R,k,l_s}^{H}\boldsymbol{g}_{k,l_s}x_{l_s}^{s} \\ &+ \mathbf{H}_{k,MBS}\mathbf{w}_{T,k}\mathbf{w}_{R,k,l_s}^{H}\textstyle\sum_{i=1,i\neq l_s}^{L_s}\boldsymbol{g}_{k,i}x_i^{s} \\ &+ \mathbf{H}_{k,MBS}\mathbf{w}_{T,k}\mathbf{w}_{R,k,l_s}^{H}\boldsymbol{G}_{k,PU}\boldsymbol{x}_p \\ &+ \mathbf{H}_{k,MBS}\mathbf{w}_{T,k}\mathbf{w}_{R,k,l_s}^{H}\boldsymbol{n}_{k,SBS},\end{aligned} \tag{10}$$

When the MBS applies the output of the array, $\boldsymbol{y}_{MBS}$, to the hybrid weight, $\boldsymbol{c}_k^{H}$, the detection of the l_s^{th} user signal of the k^{th} SBS by the MBS can be expressed as

$$\hat{x}_{k,l_s} = \boldsymbol{c}_k^{H}\boldsymbol{y}_{\text{MBS}} = \boldsymbol{c}_k^{H}\left(\mathbf{S}_{k,l_s} + \mathbf{S}_I^{SBSs} + \mathbf{S}_{k,I}^{SU} + \mathbf{S}_I^{\text{PU}} + \boldsymbol{N}_{MBS}\right)\ , \tag{11}$$

where

$\mathbf{S}_{k,l_s} = \mathbf{H}_{k,MBS}\mathbf{w}_{T,k}\mathbf{w}_{R,k,l_s}^{H}\mathbf{g}_{k,l_s}x_{l_s}^{s}$ is the l_s^{th} user signal of the k^{th} SBS,
$\mathbf{S}_{k,I}^{\text{SU}} = \mathbf{H}_{k,MBS}\mathbf{w}_{T,k}\mathbf{w}_{R,k,l_s}^{H}\sum_{i=1,i\neq l_s}^{L_s}\boldsymbol{g}_{k,i}x_i^{s}$ is the interference from the $L_s - 1$ other SUs of k^{th} SBS,
$\mathbf{S}_I^{SBS} = \sum_{i=1,\ i\neq k}^{K}\left(\mathbf{H}_{i,MBS}\mathbf{w}_{T,i}\mathbf{w}_{R,i,l_s}^{H}\boldsymbol{y}_{i,SBS}\right)$ is the interference from the $K - 1$ other SBSs.
$\mathbf{S}_I^{\text{PU}} = \mathbf{H}_{k,MBS}\mathbf{w}_{T,k}\mathbf{w}_{R,k,l_s}^{H}\boldsymbol{G}_{k,PU}\boldsymbol{x}_p + \boldsymbol{c}_k^{H}\mathbf{H}_{PU,MBS}\boldsymbol{x}_p$
$\boldsymbol{N}_{MBS} = \left(\mathbf{H}_{k,MBS}\mathbf{w}_{T,k}\mathbf{w}_{R,k,l_s}^{H}\boldsymbol{n}_{k,SBS} + \boldsymbol{n}_{MBS}\right)$

The end-to-end SINR at the MBS for the l_s^{th} user of the k^{th} SBS can be expressed as

$$\gamma_{k,l_s}^{MBS} = \frac{\boldsymbol{c}_{\text{k}}^{H}\mathbf{H}_{k,MBS}\mathbf{w}_{T,k}\mathbf{w}_{R,k,l_s}^{H}\boldsymbol{g}_{k,l_s}x_{l_s}^{s}\left(x_{l_s}^{s}\right)^{H}\boldsymbol{g}_{k,l_s}^{H}\mathbf{w}_{R,k,l_s}\mathbf{w}_{T,k}^{H}\mathbf{H}_{k,MBS}^{H}\boldsymbol{c}_k}{\mathbf{c}_{\text{k}}^{H}\mathbf{B}_{AL-BL}\boldsymbol{c}_k}\ , \tag{12}$$

where $\mathbf{B}_{AL-BL} = \mathbf{S}_{k,I}^{\text{SU}}\left(\mathbf{S}_{k,I}^{\text{SU}}\right)^{H} + \mathbf{S}_I^{SBS}\left(\mathbf{S}_I^{SBS}\right)^{H} + \mathbf{S}_I^{\text{PU}}\left(\mathbf{S}_I^{\text{PU}}\right)^{H} + \boldsymbol{N}_{MBS}(\boldsymbol{N}_{MBS})^{H}$ is the covariance matrix of the interference-plus-noise for the l_s^{th} user end-to-end link.

The ergodic channel capacity for each user, l_s, is given by [19]

$$\mathcal{C} = \mathbb{E}\left(log_2\left\{1 + \frac{\boldsymbol{c}_{\text{k}}^{H}\mathbf{H}_{k,MBS}\mathbf{w}_{T,k}\mathbf{w}_{R,k,l_s}^{H}\boldsymbol{g}_{k,l_s}\boldsymbol{x}_s\boldsymbol{x}_s^{H}\boldsymbol{g}_{k,l_s}^{H}\mathbf{w}_{R,k,l_s}\mathbf{w}_{T,k}^{H}\mathbf{H}_{k,MBS}^{H}\boldsymbol{c}_k}{\mathbf{c}_{\text{k}}^{H}\mathbf{B}_{AL-BL}\boldsymbol{c}_k}\right\}\right)\ , \tag{13}$$

where $\mathbb{E}(.)$ denotes the expectation operator.

2.4. Channel Model

For the access and backhaul links, we consider mmWave propagation channels with limited scattering which can be modelled at each subcarrier by the clustered channel representation [13]. We assume a scattering environment with N_{cl} scattering clusters randomly distributed in space and within each cluster, there are N_{ray} closely located scatterers.

For the backhaul link, the channel matrix at subcarrier f_n between the k^{th} SBS and the MBS can be expressed as

$$\mathbf{H}_{k,MBS,f_n} = \sqrt{\frac{N_a M_a}{N_{cl} N_{ray}}} \sum_{i}^{N_{cl}} \sum_{l=1}^{N_{ray}} \alpha_{il,f_n} \boldsymbol{a}_{MBS,f_n}\left(\varnothing_{i,l}^{r}, \theta_{i,l}^{r}\right) \boldsymbol{a}_{k,SBS,f_n}^{*}\left(\varnothing_{i,l}^{t}, \theta_{i,l}^{t}\right), \tag{14}$$

where $\alpha_{il,f_n} = \widetilde{\alpha}_{il} e^{-j2\pi i f_n / N_c}$ are the complex gains of the j^{th} ray in the i^{th} scattering cluster and $\widetilde{\alpha}_{il}$ are assumed i.i.d $\text{CN}(0, \sigma_{\widetilde{\alpha},i}^2)$. With $\sigma_{\widetilde{\alpha},i}^2$ representing the average power of the i^{th} cluster, $\varnothing_{i,l}^{r}$ and $\varnothing_{i,l}^{t}$ are the azimuth angles of arrival and departure, respectively, $\theta_{i,j}^{r}$ *and* $\theta_{i,j}^{t}$ are the elevation angles of arrival and departure, respectively, and $\boldsymbol{a}_{MBS,f_n}\left(\varnothing_{i,l}^{r}, \theta_{i,l}^{r}\right)$ and $\boldsymbol{a}_{k,SBS,f_n}\left(\varnothing_{i,l}^{t}, \theta_{i,l}^{t}\right)$ represent, respectively, the normalized receive and transmit array response vectors of the MBS and the k^{th} SBS.

For the access link, the channel matrix at subcarrier f_n between the k^{th} SBS and its L_s users can be written as

$$\boldsymbol{G}_{k,SU,f_n} = \sqrt{\frac{L_s M_a}{N_{cl} N_{ray}}} \sum_{i}^{N_{cl}} \sum_{l=1}^{N_{ray}} \alpha_{il,f_n} \boldsymbol{a}_{SBS,f_n}\left(\varnothing_{i,l}^{r}, \theta_{i,l}^{r}\right) \boldsymbol{a}_{k,SU,f_n}^{*}\left(\varnothing_{i,l}^{t}, \theta_{i,l}^{t}\right), \tag{15}$$

where $\boldsymbol{a}_{k,SU,f_n}\left(\varnothing_{i,l}^{t}, \theta_{i,l}^{t}\right)$ represents the spatial signature vector of the L_s single antenna users.

The N_{ray} azimuth and elevation angles, $\varnothing_{i,l}^{r,t}$ and $\theta_{i,l}^{r,t}$, within the cluster i are assumed to be randomly distributed with a uniformly-random mean cluster angle of $\varnothing_{i}^{r,t}$ *and* $\theta_{i}^{r,t}$, respectively, and a constant angular spread of $\sigma_{\varnothing^{r,t}}$ *and* $\sigma_{\theta^{r,t}}$, respectively.

For simplicity, the access links between the MBS and its L_p users ($\mathbf{H}_{PU,MBS}$) and between PUs and the k^{th} SBS ($\boldsymbol{G}_{k,PU}$) are modeled by convetional i.i.d MIMO channels.

Note that in this per-subcarrrier representation, it is assumed that for each subcarrier f_n , the carrier frequency f_c is much larger than $f_c \pm f_n$ and that $\boldsymbol{a}_{MBS,f_n}\left(\varnothing_{i,l}^{r}, \theta_{i,l}^{r}\right)$ and $\boldsymbol{a}_{k,SBS,f_n}\left(\varnothing_{i,l}^{t}, \theta_{i,l}^{t}\right)$ can approximately be considered equal for all subcarriers. Consequently, the channel covariance matrices are approximately similar with the same set of eigenvectors for all subcarriers and can be replaced by the average of the covariance matrices, i.e., $\mathbf{H}_{AL,k,l_s}^{H}\mathbf{H}_{AL,k,l_s} = \frac{1}{N_c}\sum_{n=1}^{N_c}\mathbf{H}_{AL,k,l_s,f_n}^{H}\mathbf{H}_{AL,k,l_s,f_n}$, $\mathbf{H}_{BL,k}^{H}\mathbf{H}_{BL,k} = \frac{1}{N_c}\sum_{n=1}^{N_c}\mathbf{H}_{BL,k,f_n}^{H}\mathbf{H}_{BL,k,f_n}$, and $\mathbf{H}_{PU,MBS}^{H}\mathbf{H}_{PU,MBS} = \frac{1}{N_c}\sum_{n=1}^{N_c}\mathbf{H}_{PU,MBS,f_n}^{H}\mathbf{H}_{PU,MBS,f_n}$.

3. Proposed Hybrid Beamforming

3.1. Access Link

The k^{th} SBS communicates with each SU through a set of selected beams that corresponds to a set of weight vectors. These weight vectors are obtained using the eigenbeamforming scheme and can be expressed as

$$\begin{gathered} \boldsymbol{A}_{R,k,l_s}^{SBS} = \left[\boldsymbol{a}_{R,k,l_s,1}^{SBS}, \boldsymbol{a}_{R,k,l_s,2}^{SBS}, \cdots, \boldsymbol{a}_{R,k,l_s,N_d}^{SBS}\right] \\ subject\ to\ \left|\boldsymbol{A}_{R,k,l_s}^{SBS}(i,j)\right|^2 = 1 \end{gathered}, \tag{16}$$

where $\boldsymbol{a}_{R,k,l_s,i}^{SBS}$ denote the i^{th} selected $M_a \times 1$ eigenvector corresponding to the i^{th} maximum eigen value of $\boldsymbol{g}_{k,l_s}^{H}\boldsymbol{g}_{k,l_s}$.

Since the analog beamforming matrix $\boldsymbol{A}_{R,k,l_s}^{SBS}$ is realized using phase shifters only, its elements, $\boldsymbol{A}_{R,k,l_s}^{SBS}(i,j)$, satisfy $\left|\boldsymbol{A}_{R,k,l_s}^{SBS}(i,j)\right|^2 = 1$. It should be noted that each SBS is using a different analog matrix for each user and that the system model shown in Figure 1 focuses on the detection of the l_s^{th} user of the k^{th} SBS and shows the analog beamformer and the RF chains for one user only. The analog beamformer can be implemented using the Butler matrix as shown in Figure 4, where four users $(L_s = 4)$ and four RF chains per user $(N_d = 4)$ are assumed. Depending upon which 4 ports are activated, 4 beams are produced in specified directions. Since we are assuming 4 different channels, we should expect 4 different ports for each user.

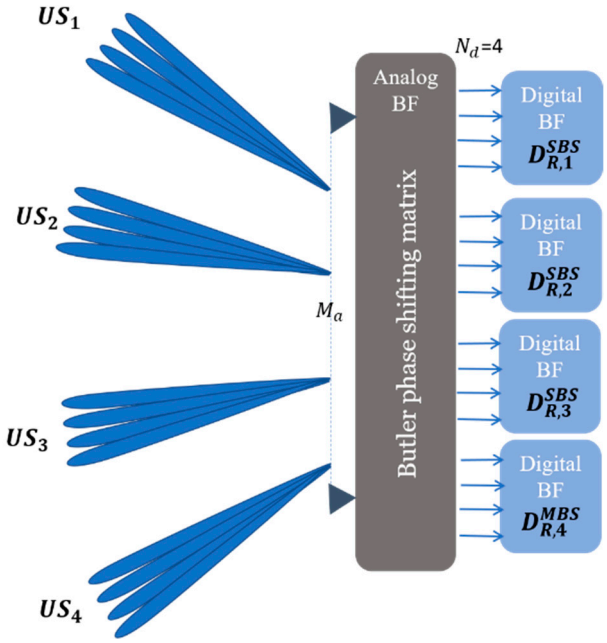

Figure 4. Hybrid beamforming based on Butler matrix for the access link.

Once the analog beams are selected, the received optimal digital weights, $\boldsymbol{D}_{R,k,l_s}^{SBS}$, are obtained based on the maximization of the access link receive SINR, γ_{k,l_s}^{SBS}, given by Equation (3):

$$\boldsymbol{D}_{R,k,l_s}^{SBS} = \boldsymbol{B}_{AL,k,l_s}^{-1}\boldsymbol{V}_{AL,k,l_s}\,, \tag{17}$$

where $\boldsymbol{V}_{AL,k,l_s}$ denote the eigen vector corresponding to the maximum eigenvalue of the effective access channel, $\boldsymbol{H}_{AL,k,l_s}^{H}\boldsymbol{H}_{AL,k,l_s}$.

3.2. Backhaul Link

The transmit analog weights of the k^{th} SBS are based on the eigenbeamforming scheme and are given by

$$\begin{gathered}\boldsymbol{A}_{T,k}^{SBS} = \left[\boldsymbol{a}_{T,k,1}^{SBS}, \boldsymbol{a}_{T,k,2}^{SBS}, \cdots, \boldsymbol{a}_{T,k,N_d}^{SBS}\right] \\ subject\ to\ \left|\boldsymbol{A}_{T,k}^{SBS}(i,j)\right|^2 = 1\end{gathered}\,, \tag{18}$$

where $\boldsymbol{a}_{T,k,i}^{SBS}$ denote the i^{th} selected $N_a \times 1$ eigenvector corresponding to the i^{th} maximum eigenvalue of $\boldsymbol{H}_{k,\text{MBS}}^{H}\boldsymbol{H}_{k,\text{MBS}}$.

Assuming channel reciprocity with $N_a = M_a$, the receive analog weight vectors of the MBS are given by $\boldsymbol{A}_{R,k}^{MBS} = \boldsymbol{A}_{T,k}^{SBS}$. It should also be noted that the MBS is using a different analog matrix for each SBS, which can be implemented using the Butler matrix of Figure 4, where mobile users are replaced by SBSs.

For fixed analog beamforming weights, $\boldsymbol{A}_{T,k}^{SBS}$ and $\boldsymbol{A}_{R,k}^{MBS}$, the transmit optimal digital weight vector of the k^{th} SBS, $\boldsymbol{D}_{T,k}^{SBS}$, and the receive optimal digital weight vector of the MBS, $\boldsymbol{D}_{R,k}^{MBS}$, are obtained base on the maximization of the backhaul link receive SINR and are given by

$$\boldsymbol{D}_{T,k}^{SBS} = \boldsymbol{D}_{R,k}^{MBS} = \boldsymbol{B}_{BL,k}^{-1} \boldsymbol{H}_{\boldsymbol{BL,k}} \boldsymbol{V}_{BL} \,, \tag{19}$$

where $\boldsymbol{V}_{BL}$ is the eigenvector corresponding to the maximum eigenvalue of $\mathbf{H}_{BL,k}^{H} \mathbf{H}_{BL,k}$, with $\boldsymbol{H}_{BL,k}$ representing the effective channel given by $\boldsymbol{H}_{BL,k} = \left(\boldsymbol{A}_{\boldsymbol{R}}^{\boldsymbol{MBS}}\right)_{k}^{H} \mathbf{H}_{k,MBS} \left(\boldsymbol{A}_{\boldsymbol{T}}^{\boldsymbol{SBS}}\right)_{k}^{H}$.

4. Simulation Results

In our simulation setups, we considered a HetNet organized into four SBSs ($K = 4$) and one macro-cell. The SBSs and the MBS used the same number of antennas, $N_a = M_a = 64$, and the same number of RF chains, $N_d = M_d = 2$ *or* 4. Each SBS is serving $L_s = 4$ users and the macro-cell is serving 4 users, each transmitting with a single antenna. We assumed QPSK modulation. For the OFDM configurations, we assumed the 256-OFDM system ($N_c = 256$), which is widely deployed in broadband wireless access services.

Figure 5 shows the beampattern of the proposed HBF with four RF chains and the optimal fully-digital one for the access link. It is noted that the optimal beamformer has about five dominant beams, three of which are similar to the selected beams of the proposed HBF. This beampattern means that the data streams can be successfully transmitted through those three beams using the proposed HBF and that near optimal performance could be achieved if we were to bring the number of RF chains close to the number of dominant beams of the optimal beamformer. For the backhaul link, Figure 6 shows very similar beampatterns with more dominant beams.

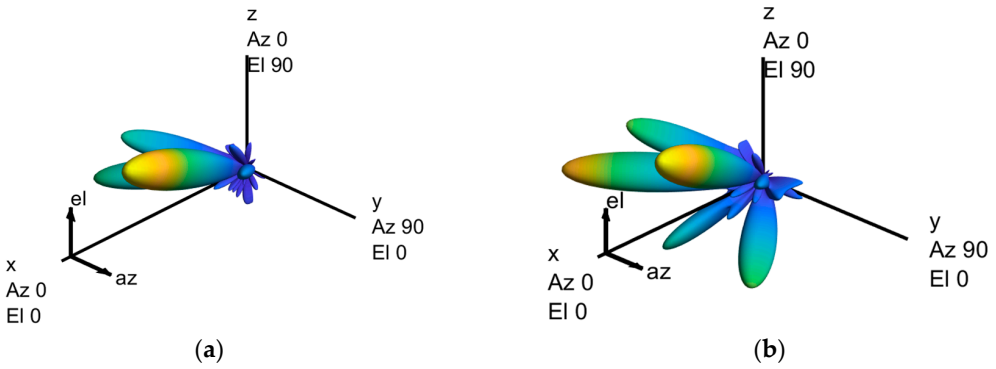

Figure 5. Beampattern of the access link: (**a**) Proposed HBF, 4 RF chains; (**b**) fully-digital beamforming (optimal).

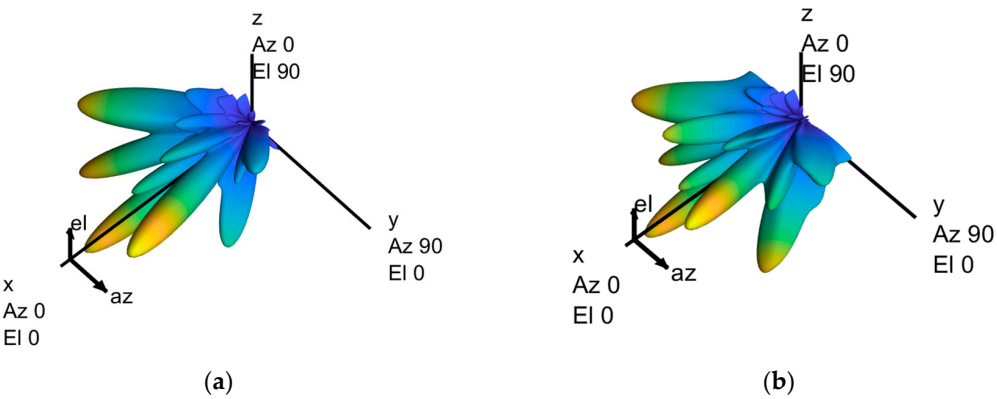

Figure 6. Beampattern of the backhaul link: (**a**) Proposed HBF, 4 RF chains; (**b**) fully-digital beamforming (optimal).

Figure 7, on the other hand, compares the ergodic channel capacity of the proposed HBF and the optimal fully-digital one. It is observed that for both cases the optimal beamformer is outperforming the proposed HBF. However, as we increase the number of RF chains, the performance gap between the two schemes was reduced, and a near-optimal solution was achieved by the proposed HBF using four RF chains. On the other hand, for the single cell MU-MIMO case presented in References [12–14], near optimal performance was achieved with only five RF chains, and for the MU-MIMO case in [16,17], it was shown that the required number RF chains could be reduced to two to achieve fully digital beamforming performance. However, unlike our case, where we have assumed a HetNet with a macro cell and multiple small cognitive cells, these studies focused primarily on macro-cellular systems and did not consider HBF in the context of HetNets.

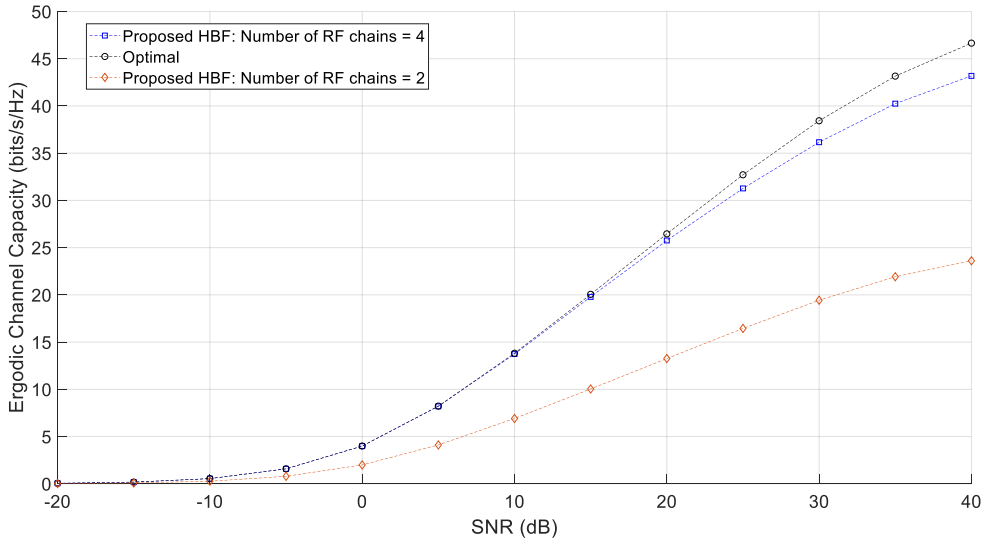

Figure 7. Ergodic channel capacity of the proposed HBF for different number of RF chains.

5. Conclusions

In this paper, we employed hybrid beamforming at the access and backhaul links of a mmWave HetNet system. We proposed a low-complexity HBF that was fully-based on MRT/MRC Eigen-beamforming schemes. The performance evaluation in terms of the beam patterns and the ergodic channel capacity showed that the proposed HBF scheme achieved near-optimal performance with only four RF chains and required considerably less computational complexity.

Funding: This research received no external funding.

Acknowledgments: The author would like to thank the Canadian Microelectronics Corporation (CMC) for providing the Heterogeneous Parallel Platform to run the computationally-intensive Monte-Carlo Simulations.

Conflicts of Interest: The authors declare no conflict of interest.

References

1. Siddique, U.; Tabassum, H.; Hossain, E.; Kim, D.I. Wireless backhauling of 5G small cells: Challenges and solution approaches. *IEEE Wirel. Commun.* **2015**, *22*, 22–31. [CrossRef]
2. Gao, Z.; Dai, L.; Mi, D.; Wang, Z.; Imran, M.A.; Shakir, M.Z. MmWave Massive MIMO Based Wireless Backhaul for 5G Ultra-Dense Network. *IEEE Wirel. Commun.* **2015**, *22*, 13–21. [CrossRef]
3. Tabassum, H.; Hamdi, S.A.; Hossai, E. Analysis of massive MIMO-enabled downlink wireless backhauling for full-duplex small cells. *IEEE Trans. Commun.* **2016**, *64*, 2354–2369. [CrossRef]
4. Shariat, M.; Pateromichelakis, E.; Quddus, A.; Tafazolli, R. Joint TDD Backhaul and Access Optimization in Dense Small-Cell Networks. *IEEE Trans. Veh. Technol.* **2015**, *64*, 5288–5299. [CrossRef]
5. ElSawy, H.; Hossain, E.; Kim, D.I. HetNets with cognitive small cells: User offloading and Distributed channel allocation techniques. *IEEE Commun. Mag.* **2013**, *51*, 28–36. [CrossRef]

6. Yan, Z.; Zhou, W.; Chen, S.; Liu, H. Modeling and Analysis of Two-Tier HetNets with Cognitive Small Cells. *IEEE Access.* **2016**, *5*, 2904–2912. [CrossRef]
7. Marzetta, T.L. Noncooperative cellular wireless with unlimited numbers of base station antennas. *IEEE Trans. Wirel. Commun.* **2010**, *9*, 3590–3600. [CrossRef]
8. Rusek, F.; Persson, D.; Lau, B.; Larsson, E.; Marzetta, T.L.; Edfors, O.; Tufvesson, F. Scaling up MIMO: Opportunities and challenges with very large arrays. *IEEE Signal Process. Mag.* **2013**, *30*, 40–60. [CrossRef]
9. Ngo, H.Q.; Larsson, E.G.; Marzetta, T.L. Energy and spectral efficiency of very large multiuser MIMO systems. *IEEE Trans. Commun.* **2013**, *61*, 1436–1449.
10. Hoydis, J.; ten Brink, S.; Debbah, M. Massive MIMO in the UL/DL of cellular networks: How many antennas do we need? *IEEE J. Sel. Areas Commun.* **2013**, *31*, 160–171. [CrossRef]
11. Hefnawi, M. Capacity-Aware Multi-User Massive MIMO for Heterogeneous Cellular Network. In Proceedings of the IEEE International Conference on Selected Topics in Mobile and Wireless Networking, Tangier, Morocco, 20–22 June 2018.
12. Sohrabi, F.; Yu, W. Hybrid beamforming with finite-resolution phase shifters for large-scale MIMO systems. In Proceedings of the IEEE Workshop Signal Processing Advances in Wireless Communications, Stockholm, Sweden, 28 June–1 July 2015.
13. El Ayach, O.; Rajagopal, S.; Abu-Surra, S.; Pi, Z.; Heath, R. Spatially sparse precoding in millimeter wave MIMO systems. *IEEE Trans. Wirel. Commun.* **2014**, *13*, 1499–1513. [CrossRef]
14. Alkhateeb, A.; El Ayach, O.; Leus, G.; Heath, R. Channel estimation and hybrid precoding for millimeter wave cellular systems. *IEEE J. Sel. Top. Signal Process.* **2014**, *8*, 831–846. [CrossRef]
15. Sohrabi, F.; Yu, W. Hybrid digital and analog beamforming design for large-scale MIMO systems. In Proceedings of the IEEE International Conference on Acoustics, Speech, Signal Process (ICASSP), Brisbane, Australia, 19–24 April 2015.
16. Liang, L.; Dai, Y.; Xu, W.; Dong, X. How to approach zero-forcing under RF chain limitations in large mmwave multiuser systems? In Proceedings of the IEEE/CIC International Conference on Communications in China, Shanghai, China, 13–15 October 2014.
17. Liang, L.; Xu, W.; Dong, X. Low-complexity hybrid precoding in massive multiuser MIMO systems. *IEEE Wirel. Commun.* **2014**. [CrossRef]
18. Kang, M. A comparative study on the performance of MIMO MRC systems with and without cochannel interference. *IEEE Trans. Commun.* **2004**, *52*, 1417–1425. [CrossRef]
19. Sulyman, A.I.; Hefnawi, M. Adaptive MIMO Beamforming Algorithm Based on Gradient Search of the Channel Capacity in OFDMSDMA System. *IEEE Commun. Lett.* **2008**, *12*, 642–644. [CrossRef]